



University of Molise

Department of Biosciences and Territory

Bachelor Thesis

Global and Local Prediction in Automatic detection of Atrial Fibrillation

Alex Colucci

December, 2019

Supervisor
Prof. Oliveto Rocco

Co-Supervisor
Gennaro Laudato PhD

*“It does not matter where you go and what you study, what matters most is
what you share with yourself and the world.”*

Santosh Kalwar

*Dedicated to my family, my friends and all the people who have
accompanied me on this journey and allowed me to grow.*

Contents

| | | |
|----------|--|-----------|
| 1 | Introduction | 1 |
| 1.1 | Application context | 1 |
| 1.2 | Motivations & Objectives | 4 |
| 1.3 | Results achieved | 5 |
| 1.4 | Structure of the thesis | 5 |
| 2 | State of the art | 7 |
| 2.1 | Introduction | 7 |
| 2.2 | Methods of the literature | 7 |
| 2.3 | The best approach proposed in the literature | 8 |
| 2.4 | Results and comparisons | 9 |
| 3 | Improving global prediction with morphological features | 11 |
| 3.1 | Approach description | 11 |
| 3.1.1 | Features description | 11 |
| 3.1.2 | Machine learning techniques | 12 |
| 3.2 | Empirical evaluation | 12 |
| 3.2.1 | Design & Context | 12 |
| 3.2.2 | Results | 14 |
| 3.3 | Most significant features | 15 |
| 3.4 | Final remarks | 16 |
| 3.4.1 | Results without morphology | 16 |
| 4 | An adaptive and local prediction approach | 23 |
| 4.1 | Approach description | 23 |
| 4.2 | Empirical evaluation | 23 |
| 4.2.1 | Design & Context | 23 |
| 4.2.2 | Results | 24 |
| 4.3 | Final remarks | 24 |

| | | |
|----------|-------------------------|-----------|
| 5 | Conclusions | 27 |
| 5.1 | Final remarks | 27 |
| 5.2 | Future works | 27 |

List of Figures

| | | |
|-----|--|----|
| 1.1 | A normal heartbeat on the left, and AF heartbeat on the right. Image from mayoclinic.org | 1 |
| 1.2 | Cardiac cycle divided into different components. P , QRS and T | 3 |
| 1.3 | ECG of a heart with atrial fibrillation on top and with normal sinus rhythm on the bottom. | 4 |
| 2.1 | Application of the method to detect AF. (a) is the original sequence hr_n ; (b) is the symbolic dynamic syn ; (c) the word sequence wn_n ; (d) the distribution of $\mathcal{H}''(\mathbf{A})$ | 8 |
| 4.1 | Example of optimisation through ROC. For the record 05091, the best performance is obtained with threshold 0.046. $Se = 0.90$ and $Sp = 0.82$ | 24 |

List of Tables

| | | |
|-----|--|----|
| 2.1 | Performance comparison of some state of the art methods. | 9 |
| 3.1 | State of the art algorithm replication performance. | 13 |
| 3.2 | The number of beats comparison between state of the art and replication. | 13 |
| 3.3 | Machine learning algorithms applied on the dataset with Fast Fourier Transform and AR coefficients, compared with the replication of Zhou and Zhou, et al [17] itself. | 15 |
| 3.4 | Most significant features on the dataset based on entropy with FFT and AR coefficients. Rank found with correlation attribute evaluation. | 16 |
| 3.5 | Machine learning algorithms applied on the dataset with explicit and encoded entropy, compared with the replication of Zhou and Zhou, et al [17] itself. | 17 |
| 3.6 | Machine learning algorithms applied on the dataset with explicit and encoded entropy without the transient beats, compared with the replication of Zhou and Zhou, et al [17, p. 7] itself. | 18 |
| 3.7 | Part 1: Records with specific improvements of classification based on encoded entropy with FFT experiment. | 19 |
| 3.8 | Part 2: Records with specific improvements of classification based on encoded entropy with FFT experiment. | 20 |
| 3.9 | Part 3: Records with specific improvements of classification based on encoded entropy with FFT experiment. | 21 |
| 4.1 | Summary of local prediction best threshold per record. | 25 |
| 4.2 | GLS function applied on a dataset with a window of the first 30 AF beats. The output of the function is a threshold. | 25 |

Chapter 1

Introduction

1.1 Application context

In this section, the most dangerous heart disease is analysed and described by providing information on classification, causes, symptoms and different methods of diagnosis with a particular focus on the electrocardiogram.

Atrial fibrillation, also abbreviated with AF or A-Fib, is an abnormal heart rhythm that happens when electrical impulses fire off in the atria (Figure 1.1), from different spots without being organized. Characterized by rapid and irregular beating, caused by the chambers of the heart twitching [1]. This arrhythmia is associated with an increased risk of stroke, in fact the proportion of strokes associated with AF increases from 6.6%, for ages 50 to 59 years, to 36.2% for ages 80 to 89 years [2]. Other risks are heart failure and even dementia [3]. The estimated number of individuals with AF globally in 2010 was 33,5 million and as the population ages globally, the burden of AF grows [4].

The disease is classified by doctors based on how long it lasts or based on

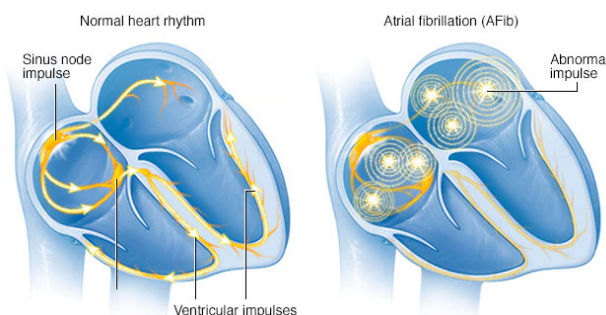


Figure 1.1: A normal heartbeat on the left, and AF heartbeat on the right. Image from mayoclinic.org

the cause. The treatment will be different for each kind [5]:

- **Paroxysmal** (holiday heart syndrome): an episode of AF, the duration of whose maybe a few minutes or a few days, but which tends to be below the week. Usually, treatment is not needed;
- **Persistent**: the disease lasts longer than a week and it can stop on its own, or a specific medicine or treatment is needed. If the latter does not work, doctors opt for the electrical cardioversion, which is a low-voltage current used to reset the normal rhythm;
- **Permanent**: also called chronic, cannot be treated. The doctor decides for a long term medication to reduce the odds of associated health conditions.

There are many possible causes of the condition, some are controllable, others are not. Cardiovascular factors play a big role: high blood pressure, heart valve disease, congenital heart disease and even previous heart surgery. But difficulties in breathing are a key factor too, in other words, obesity and obstructive sleep apnea [6]. Alcohol consumption and tobacco smoking are associated with an increased risk of developing atrial fibrillation [7, 8]. Other factors are genetics, ageing, a sedentary lifestyle and diabetes [9, 10]. The person often feels an abnormal beating that starts to become longer and constant. There could be heart palpitations, shortness of breath, chest pain, light-headedness, or fainting [11]. But the biggest problem is that often these kind of episodes are asymptomatic [3], in fact sometimes first diagnosed when patients present a stroke [12].

A doctor to diagnose AF could check your signs and symptoms, together with your medical history and conduct a different kind of tests [13]:

- **Electrocardiogram** (ECG or EKG) is the process through which a recording of the electrical activity of the patient's heart is made. To measure the electrical signals as they travel, multiple small sensors, called electrodes, are attached to the body. This test plays a key role among all the other tools used. A more in-depth explanation will be offered in Section 1.1.
- **Holter monitor** is a portable ECG device that can be carried in a pocket or even worn on a shoulder strap or a belt. The monitor will check the heart's activity for 24 hours, sometimes even longer. It is a common practice to utilize the device when there is a strong suspect about a Paroxysmal-AF but an ECG during an office visit detects only a regular rhythm.

1.1. APPLICATION CONTEXT

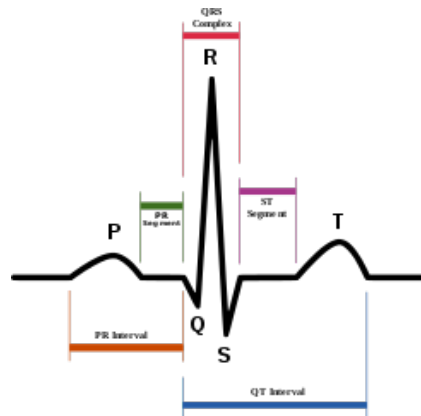


Figure 1.2: Cardiac cycle divided into different components. P , QRS and T .

- **Event recorder** is another kind of ECG portable device that is meant to monitor the heartbeat over a few weeks to a few months. When the patient feels a symptom, then the button should be pressed to let the device memorize an ECG strip of the preceding few minutes and following few minutes.
- **Echocardiogram** is a non-invasive test that uses ultrasound waves to scan the heart and get moving pictures of the organ. The doctors aim to find problems in the valves, in the size of the left and right atrial or more general structural heart disease or blood clots.
- **Blood tests** are used to check any thyroid problems or other substances in the patient's blood that may lead to AF.
- **Stress test** can help the doctor in the task of finding AF. The reason is that some individual with the disease do well in normal activity, but not with exertion. Moreover, the nature of the symptoms can be understood.
- **Chest X-ray** help to see the condition of the lungs and heart of a specific patient. In general, it's used if a pulmonary cause of AF is suggested or if conditions like congestive heart failure are suspected.

The first type of test, the ECG, is an investigation performed routinely whenever an irregular heartbeat is suspected. And it can be done in the office and later even with a portable device, thus it's a relevant tool through which an automatic detection of atrial fibrillation can be implemented.

Electrocardiography produces an electrocardiogram (ECG), namely a recording which is a graph where the x-axis represents the time and the y-axis



Figure 1.3: ECG of a heart with atrial fibrillation on top and with normal sinus rhythm on the bottom.

represents the voltage, of the electrical activity of the heart using electrodes placed on the skin [14, p.74]. In this way, small electrical changes can be detected, that are the normal consequences of cardiac muscle depolarization followed by a re-polarization during each cardiac cycle (Figure 1.2). Normally the number of electrodes attached to the patient's limbs and on the surface of the chest is 10, this allows to form 12 ECG leads. Thus the overall magnitude of the electrical potential of the heart can be measured from twelve different angles (leads).

A single cardiac cycle can be divided into different components as in (Figure 1.2). The first is called *P* wave, which represents the depolarization of the atria. The second one is the *QRS* complex, that symbolizes the ventricles' depolarization. To finish with the *T* wave, which represents the re-polarization of the ventricles [14, p.80].

Knowing all this, to find atrial fibrillation heartbeats through the electrocardiogram is sufficient to run an investigation on the absence of *P* waves with disorganized electrical activity in their place and irregular *R – R* intervals caused by irregular conduction of impulses to the ventricles [15]. Furthermore, problems over fast heart rates arise since A-Fib may look more regular, which could make it indistinguishable from other supraventricular tachycardias or ventricular tachycardia [16]. Besides *QRS* complexes should be quite narrow because it means that they are initiated by a normal flow of electrical activity through the intraventricular conduction system. Otherwise wide complexes are disquieting for ventricular tachycardia, albeit in cases where there is a disorder with the conduction system, wide *QRS* complexes may be present in A-fib with a rapid ventricular response. A good example is shown in (Figure 1.3).

1.2 Motivations & Objectives

For the automatic detection of atrial fibrillation, several methods can be found in the literature. Some of these methods are based on the morphology

1.3. RESULTS ACHIEVED

of the ECG, others on the heart rate obtained from the signal. The state-of-the-art method Zhou et, al [17], described in Chapter 2, is based on the latter. Following a thorough analysis, two important limitations emerge:

- morphology is an important factor since AF has no P wave, i.e. a morphological characteristic, due to noise.
- using a single discriminant threshold for all patients is a strong intake.

The objectives of this twofold thesis are therefore the following.

- starting from the state of the art algorithm, try to improve the global prediction system, i.e. a unique for all the patients, by incorporating into the approach of Zhou et, al morphological features.
- starting from the state of the art algorithm, realize a local prediction model, i.e. unique and adaptive for a specific patient.

1.3 Results achieved

The thesis has managed to obtain, with respect to the state of the art algorithm, an increase in performance using datasets morphologically enriched at the level of global prediction. For each specific record, it is possible to obtain remarkable improvements, especially in terms of true positives. Specifically, on the dataset with explicit entropy, tailor-made entropy and FFT improvements are obtained on MCC , SE , SP respectively equal to 8/23, 14/23, 12/23 and the number of records without improvements is 4/23. In the dataset based on explicit entropy, tailor-made entropy with FFT and AR coefficients, the results in terms of MCC , SE , SP are respectively 14/23, 22/23 and 13/23. With only one record without any improvement. As for the work on finding the optimal local threshold, the GLS model manages to predict the optimal thresholds with a small difference in most cases. For some records, thresholds are far from the optimal threshold.

1.4 Structure of the thesis

This thesis is composed of 5 chapters including this one. In particular:

- 1 Chapter 1, introduces the application context and briefly explains the reasons for the work and the results of the experimentation.

- Chapter 2 introduces the state of the art algorithm for identifying beats subject to atrial fibrillation. The thesis is based on this algorithm and shows its methodology and results.
- Chapter 3, is one of the two central parts of the work. It explains how the state of the art was improved by using machine learning techniques on morphologically enriched datasets.
- Chapter 4, the other substantial part of the work that focuses on finding an adaptive threshold for a specific patient to describe fibrillating events.
- Chapter 5, provides conclusions to the work and future developments.

Chapter 2

State of the art

2.1 Introduction

In this Chapter, an automatic approach to detect Atrial Fibrillation is analysed. The state of the art is based on different public datasets offered by PhysioNet [18], among which MIT-BIH Atrial Fibrillation Database [19] and Long Term AF Database [20] are used. The method is based on ECG, whose explanation has been given in Section 1.1. The reason that lies behind the use of ECG, is its intrinsic simplicity, that cannot be found in methods like blood tests, chest x-ray, etc.

2.2 Methods of the literature

Most of the algorithms work on the processing of the ECGs components (P wave, QRS complex, ...) and the poorly coordinate atrial activation (AA) of heart and rapid cardiac beating. Although these pieces of information can lead to the identification of Atrial Fibrillation, noise must be taken into consideration. Especially with P waves which in general is of very low-intensity magnitude. Whereas the approaches based on the RR interval (R wave peak to R wave peak) irregularity, nonetheless the component is a more prominent feature of ECG and thus less subject to noise, tend to be quite complicated and not so efficient to make them suitable for real-time applications [17, p. 2]. Examples of noteworthy methods based on RRI are the Petrénas, et al [21, 2015] and Lee, et al [22, 2013]. The former is characterized by the use of ectopic beat filtering, bigeminal suppression and signal fusion, while the latter focus on time-varying coherence functions and Shannon entropy. A real-time and low-complexity algorithm is Zhou et, al [17], based on the heart rate.

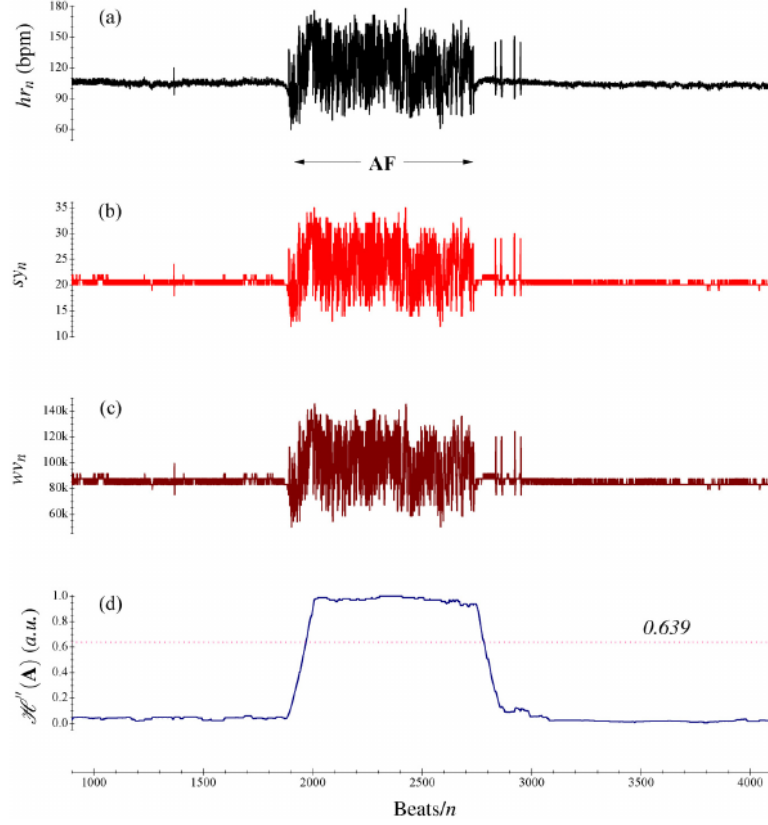


Figure 2.1: Application of the method to detect AF. (a) is the original sequence hr_n ; (b) is the symbolic dynamic sy_n ; (c) the word sequence wn_n ; (d) the distribution of $\mathcal{H}''(\mathbf{A})$.

2.3 The best approach proposed in the literature

The algorithm Zhou et, al [17] is a the base of the thesis. Hence a brief explanation of the main characteristics is needed. The method is composed of three steps defined over the heart rate sequence.

Heart rate sequence

Let hr_n be the heartbeat rate sequence obtained from,

$$hr_n = 60 \text{ s} \cdot \frac{250}{R_n - R_{n-1}} \quad (2.1)$$

where 60 are the seconds, R_n is the sequence that denotes the R peak in the QRS complex and 250 is the number of samples per second.

2.3. THE BEST APPROACH PROPOSED IN THE LITERATURE

Step 1: symbolic dynamics of hr_n sequence

Let sy_n denote a symbolic dynamics that encodes the information of hr_n to a series with fewer symbols, where the mapping function is given by [17, p. 3],

$$sy_n = \begin{cases} 63 & \text{if } hr_n \geq 315 \\ \lfloor hr_n/5 \rfloor & \text{otherwise} \end{cases} \quad (2.2)$$

where $\lfloor \cdot \rfloor$ is a floor operator. In this way the raw sequence hr_n is transformed in a sequence $sy_n \in [0, 63]$, with 64 instantaneous states (Figure 2.1 (b)).

Step 2: history sequence of sy_n

A 3-symbols template can be applied to get a window of information that acts as a history (Figure 2.1 (c)), in this case on 3 successive symbols. Through a novel operator-defined below [17, p. 3], the word value can be calculated.

$$wv_n = (sy_{n-2} \times 2^{12}) + (sy_{n-1} \times 2^6) + sy_n \quad (2.3)$$

Step 3: Shannon entropy

A coarser version of Shannon entropy is employed to discriminate the AF arrhythmias (Figure 2.1 (d)). Without loss of generality, let $\mathbf{A} = (A|P)$ denote a dynamic system. The unique elements in this set can be defined as $A = \{a_1, \dots, a_k\}$ with the interrelated probability set $P = \{p_1, \dots, p_k\}$ ($1 \leq k \leq N$), where N is the total number of elements and k are the unique elements in space \mathbf{A} . Each element a_i has the probability $p_i = N_i/N$ ($0 < p_i \leq 1, \sum_{i=1}^k p_i = 1$), where N_i is the total number of the specific element a_i in space \mathbf{A} . Hence the coarser version of Shannon entropy can be defined to quantitatively calculate the information size of wv_n ,

$$\mathcal{H}''(\mathbf{A}) = -\frac{k}{N \log_2 N} \sum_{i=1}^k p_i \log_2 p_i \quad (2.4)$$

The dynamic \mathcal{A} is characterized by a bin size of $N = 127$ consecutive word elements from wv_{n-126} to wv_n . By defining the characteristic set A and the corresponding probability set P , the entropy $\mathcal{H}''(\mathbf{A})$ can be calculated. A specific cardiac beat hr_n is labelled as AF if the coarser entropy meets or exceeds a discrimination optimal threshold equal to 0.639. The threshold was obtained through an investigation of various thresholds in the range $[0.0, 1.0]$ with an increment of 0.001 from the receiver operating characteristic (ROC) on training databases. The computational challenges that are found in the Equation 2.4 can be overcome with a pre-calculated map of $-\frac{1}{\log_2 N} p_i \log_2 p_i$ [17, p. 4].

2.4 Results and comparisons

The work under consideration measures the performances using sensitivity (Se), specificity (Sp), positive predictive value (PPV), and overall accuracy (ACC) [17, p. 6].

$$\begin{aligned} Se &= \frac{TP}{TP + FN}, & PPV &= \frac{TP}{TP + FP} \\ Sp &= \frac{TN}{TN + FP}, & ACC &= \frac{TP + TN}{TP + TN + FP + FN} \end{aligned} \quad (2.5)$$

where TP stands for true positives, TN true negatives, FP false positives and FN false negatives.

Table 2.1: Classification performance of different methods based on three different testing databases [17, p. 8].

| Method | Feature | Year | Database | Results | | | |
|---------------------|---------|------|-------------------|---------|-------|--------|--------|
| | | | | SE(%) | SP(%) | PPV(%) | ACC(%) |
| Zhou, et al[17] | HR | 2015 | AFDB | 97.37 | 98.44 | 97.89 | 97.99 |
| | | | AFDB ¹ | 97.31 | 98.28 | 97.89 | 97.84 |
| | | | AFDB ² | 98.43 | 98.46 | 97.92 | 98.45 |
| | | | MITDB | 97.83 | 87.41 | 47.67 | 88.51 |
| | | | NSRDB | NA | 99.68 | NA | NA |
| Petr nas, et al[21] | RRI | 2015 | AFDB | 97.12 | 98.28 | - | - |
| | | | AFDB ¹ | 97.1 | 98.1 | - | - |
| | | | AFDB ² | 98.0 | 98.2 | - | - |
| | | | MITDB | 97.8 | 86.4 | 47.67 | 88.51 |
| | | | NSRDB | NA | 98.6 | NA | NA |
| Zhou, et al[23] | RRI | 2014 | AFDB | 96.89 | 98.25 | 97.62 | 97.67 |
| | | | AFDB ¹ | 96.82 | 98.06 | 97.61 | 97.50 |
| | | | AFDB ² | 97.83 | 98.19 | 97.56 | 98.04 |
| | | | MITDB | 97.33 | 90.78 | 55.29 | 91.46 |
| | | | NSRDB | NA | 98.28 | NA | NA |
| Lee, et al[22] | RRI | 2014 | AFDB ² | 98.22 | 97.68 | - | 97.91 |
| | | | MITDB | 91.1 | 89.7 | - | - |
| | | | NSRDB | NA | 99.7 | NA | NA |

¹ Records 00735 and 03665 excluded.

² Records 04936 and 05091 excluded.

‘NA’ indicates not applicable because there is no beat with AF reference annotation in this database.

A complete overview of the results of the state of the art method explained and others can be found in Table 2.1. To be sure about experimentation, edge cases are needed. Hence dataset like MITDB which contains many coexisting various types of complex arrhythmias and NSRDB without any AF annotation, are perfect for this purpose. The method performs statistically better than the others [17, p. 11] with a very low computational complexity [17, p. 14].

Chapter 3

Improving global prediction with morphological features

In this chapter is shown how the work of Zhou et, al was improved using machine learning methods on datasets enriched with morphological features.

3.1 Approach description

Several types of data sets have been constructed by enriching Shannon's entropy with a custom entropy, the Fourier transform of Fourier and the AR coefficients. Subsequently, a model was used to classify beats into beats with or without atrial fibrillation.

3.1.1 Features description

Various features were used to provide information on rhythm and morphology. The work is based on the state of the art, so the Shannon entropy of Zhou et, al was used as the first rhythmic feature. It was employed in two different ways, by using explicitly the entropy itself or by using the explicit entropy compared with the discrimination threshold that gives back a binary classification (0, 1), i.e. the encoded version. Then a tailor-made entropy te_n was added with an observation window of 10 beats, defined in the following two-step:

1 step. Let hr_n be the heartbeat rate sequence. Filter the hr_n sequence by labelling beat 1 if is stable otherwise 0 or 2:

$$x_n = \begin{cases} 0, & \text{if } hr_n \leq 50 \\ 1, & \text{if } 50 < hr_n < 120 \\ 2, & \text{otherwise} \end{cases} \quad (3.1)$$

2 step. Count number of stable beats (1) in a window of 10 elements $[x_{n-9}, x_n]$:

$$te_n = \sum_{i=n-9}^n [x_i = 1] \quad (3.2)$$

As regards morphological attributes, the Fast Fourier Transform and the Autoregressive model's coefficient estimated through Yule-Walker, were applied on two blocks obtained from an ECG's *RR* segment divided in half. The former with an output of 16 values, the latter with 4 values. Finally, the label that represents the presence or absence of atrial fibrillation. Multiple datasets with a subset of attributes were used, of which the most enriched with 43 features.

3.1.2 Machine learning techniques

To perform exhaustive experimentation, it was thought to take from each family of algorithms of machine learning, one and only one algorithm. More specifically: `j48`, `ibk`, `logistic`, `bayesnet`, `adaboostm1`, `randomforest`, `reptree`. Subsequently, the training and testing phases were carried out through a Leave One Person Out (L1PO) methodology, i.e. train on $n - 1$ records, test on 1, repeated for each of the n records in the database.

3.2 Empirical evaluation

This section describes the database used and highlights the results of the replica of Zhou et, al used for comparison. Finally, the results obtained from the experiments with Machine learning are shown.

3.2.1 Design & Context

The experiment was conducted on MIT-BIH Atrial Fibrillation Database [19], a supervised dataset, which was labelled by experienced cardiologists and made available to the public from PhysioNet [18]. The database includes 25 long-term ECG recordings of patients with atrial fibrillation, which is mostly paroxysmal. Each record is 10 hours in duration and contains two

3.2. EMPIRICAL EVALUATION

ECG signals sampled at 250 samples per second with 12 – *bit* resolution over a range of ± 10 millivolts. The signals files `.dat` are available only on 23 records. But all of the records have `.atr` and `.qrs` annotations files. The former contains information about the kind of rhythm: atrial fibrillation, atrial flutter, junctional rhythm or other rhythms. The latter contains unaudited beat prepared using an automated detector and have not been corrected manually. In some cases, manually corrected beat annotations files `.qrsc` are present. The different models taken as reference in Section 3.1.2 were applied through Weka and the results obtained compared with a replica of Zhou et, al. In Table 3.1 the performance of the replication is reported.

Table 3.1: State of the art algorithm replication performance.

| Method | Database | Results | | | |
|-----------------|-------------------|---------|-------|--------|--------|
| | | SE(%) | SP(%) | PPV(%) | ACC(%) |
| Zhou, et al[17] | AFDB | 97.37 | 98.44 | 97.89 | 97.99 |
| A | AFDB | 96.03 | 97.49 | 96.59 | 96.87 |
| | AFDB ³ | 96.04 | 97.50 | 96.60 | 96.88 |
| B | AFDB | 95.99 | 97.50 | 96.60 | 96.86 |
| | AFDB ³ | 96.00 | 97.50 | 96.62 | 96.86 |
| C ⁴ | AFDB | 96.03 | 97.53 | 96.64 | 96.89 |
| | AFDB ³ | 96.04 | 97.53 | 96.66 | 96.90 |

³ File `.qrsc` (qrs complexes corrected manually) used when available.

⁴ Hybrid heartbeats rate were introduced. 584 *hr* not classified.

The predicted values were compared with an oracle. To define the matching oracle oa_n of a specific record, a binary sequence bs_k was used to keep track of the samples that are AF (bit 1) and non-AF (bit 0), between the peaks R_i and R_{i+1} . The correct labels were obtained from the `.atr` files. Then the percentage of AF bit in the interval RR was counted,

$$AF\% = \frac{\# \text{ of ones}}{RR \text{ length}} \quad (3.3)$$

In order to be able to carry out as complete trial as possible, the oracle oa_n was defined based on the percentage in three different ways:

Table 3.2: The number of beats comparison between state of the art and replication.

| Method | Database | AF | NON-AF | TOTAL | Difference from SOA* |
|-----------------|-------------------|----------|----------|---------|----------------------|
| Zhou, et al[17] | AFDB | 519687** | 701887** | 1221574 | 0 |
| B | AFDB | 516515 | 704969 | 1221484 | −90 beats |
| B | AFDB ³ | 518082 | 705013 | 1223095 | +1521 beats |

* Difference from state of the art method.

** [17, p. 9].

- Method *A*: oa_n is AF $\iff AF\% = 1$, else non-AF
- Method *B*: oa_n is AF $\iff AF\% > 0.5$, else non-AF
- Method *C*: oa_n is $AF\%$

In method *C* 584 beats were not classified, because of hybrids (not 1 and not 0). In Table 3.2 the number of AF and non-AF beats classified per method are shown. An artefact was introduced in the implementation of the algorithm or the definition of the oracle. Further investigation is needed, but the difference between the methods applied to the same database is negligible. Method *B* on the corrected AFDB was the base of the experiment.

3.2.2 Results

The results shown in this section were based on the dataset which always contained one of the two entropies from the state of the art and the custom-made entropy. Besides, FFT is added and when highlighted also the coefficients AR. Furthermore, to make the comparison between results more immediate, Matthews correlation coefficient (MCC), a measure of the quality of binary classification, was introduced

$$MCC = \frac{TP \times TN - FP \times FN}{\sqrt{(TP + FP)(TP + FN)(TN + FP)(TN + FN)}} \quad (3.4)$$

Overall results with morphology Table 3.3 shows final results of the process. First clarification to do is that some of the initial algorithms were removed for performance issues.

On the explicit dataset with FFT, the `logistic` tended to find a great number of true positives and in this case, it reached its best performance in terms of *SE* that was equal to 97.00%, facilitated by a dataset richer in information.

On the encoded FFT dataset, the state of the art is exceeded with an increment in terms of *MCC* equal to (+0.06) with the `adaboostm1`.

In the last case, coefficients of the autoregressive model were used in addition to FFT over the explicit dataset. A general increment over the explicit FFT, in the worst-performing algorithms was achieved, but the `logistic` decreased of (−0.21) in terms of *MCC* and the `adaboostm1` remained completely unchanged.

3.3. MOST SIGNIFICANT FEATURES

Specific results with morphology Tables 3.7, 3.8 and 3.9 show the results per record for the dataset based on encoded entropy with FFT. If the total results represent a marginal increase, then with the results per record it is possible to perceive the improvement. The number of records that improve over the Zhou et, al, was 8/23 in terms of *MCC*. The number of increments in term of *SE* was 14/23 while for the *SP* the increment was on 12/23 records. Even if when there were increments on the first metric, the number of algorithms that can better classify the true positives was higher than in the case of the second metric. To finish the number of records without any increase in performance was equal to 4/23.

In the case of the dataset based on explicit entropy with FFT the improvements over Zhou et, al in terms of *MCC*, *SE*, *SP* are respectively 13/23, 22/23 and 11/23. There is only one record without any improvement.

For the last case, the dataset based on explicit entropy with FFT and AR coefficients, the results in terms of *MCC*, *SE*, *SP* are respectively 14/23, 22/23 and 13/23. An increment compared to the version without AR coefficients.

Table 3.3: Machine learning algorithms applied on the dataset with Fast Fourier Transform and AR coefficients, compared with the replication of Zhou and Zhou, et al [17] itself.

| Dataset | Algorithm | Results | | | | |
|----------------------|--------------------|--------------|--------------|--------------|--------------|--------------|
| | | SE(%) | SP(%) | PPV(%) | ACC(%) | MCC(%) |
| Explicit FFT | j48 | 84.38 | 95.48 | 93.88 | 90.47 | 80.93 |
| | logistic | 97.00 | 95.73 | 94.92 | 96.30 | 92.56 |
| | adaboostm1 | 95.49 | 97.06 | 96.39 | 96.35 | 92.63 |
| | randomforest | 88.78 | 96.82 | 95.83 | 93.19 | 86.36 |
| | reptree | 84.82 | 95.06 | 93.39 | 90.44 | 80.82 |
| Encoded FFT | j48 | 89.01 | 93.36 | 91.68 | 91.40 | 82.61 |
| | logistic | 96.27 | 96.61 | 95.89 | 96.46 | 92.85 |
| | adaboostm1 | 95.97 | 97.26 | 96.65 | 96.68 | 93.29 |
| | randomforest | 92.44 | 94.95 | 93.78 | 93.82 | 87.51 |
| | reptree | 90.85 | 93.40 | 91.89 | 92.25 | 84.34 |
| Explicit FFT with AR | j48 | 86.74 | 94.96 | 93.40 | 91.25 | 82.40 |
| | logistic | 96.85 | 95.66 | 94.83 | 96.19 | 92.35 |
| | adaboostm1 | 95.49 | 97.06 | 96.39 | 96.35 | 92.63 |
| | randomforest | 92.30 | 97.18 | 96.42 | 94.98 | 89.89 |
| | reptree | 89.86 | 95.23 | 93.94 | 92.81 | 85.49 |
| AFDB ¹ | replication | 95.94 | 97.23 | 96.61 | 96.65 | 93.23 |

¹ Records 00735 and 03665 excluded.

‘NA’ indicates not applicable because there the metric is not offered by the reference [17].

3.3 Most significant features

An analysis to identify and evaluate the goodness of the attributes was carried out on the dataset with explicit entropy and AR coefficient and FFT. The

CHAPTER 3. IMPROVING GLOBAL PREDICTION WITH MORPHOLOGICAL FEATURES

results of the analysis of the Principal components in conjunction with a Ranker searcher, are reported in Table 3.4. The first place was occupied by entropy, then a large number of components FFT and finally an AR coefficient can be found. All the FFT and AR coefficients on block number 2. The others feature were not reported, because of the low-rank score.

Table 3.4: Most significant features on the dataset based on entropy with FFT and AR coefficients. Rank found with correlation attribute evaluation.

| Rank | Order | Attribute |
|---------|-------|------------------------------|
| 0.9274 | 1 | zhou et, al explicit entropy |
| 0.1915 | 2 | taylor-made entropy |
| 0.14502 | 26 | fft8 block2 |
| 0.14502 | 28 | fft10 block2 |
| 0.14088 | 25 | fft7 block2 |
| 0.14088 | 29 | fft11 block2 |
| 0.13726 | 27 | fft9 block2 |
| 0.12276 | 24 | fft6 block2 |
| 0.12276 | 30 | fft12 block2 |
| 0.11121 | 40 | ar2 block2 |

3.4 Final remarks

It is possible to see how a general improvement at a global level can be achieved through the addition of morphological components. On a good number of them, great improvements are obtained, which unfortunately are minimized at the level of final metrics. Moreover, since in the 3.3 section entropy was found to be of great importance, an experiment on a dataset with explicit, implicit entropy and both were proposed.

3.4.1 Results without morphology

In the case of the explicit dataset (with tailor-made entropy), the overall performance was lower than in the case of the replication. But an outstanding increment was obtained in the case of the `logistic` algorithm in term of *SE* around (+0.92). The *MCC* though of the `logistic` was quite low compared to the replica. All in all, the expected result, since the threshold was not used to discriminate against the Shannon entropy.

As for the encoded case, an increase in performance was hypothesised, which proved to be true. Five out of seven algorithms were able to obtain an increase in *MCC* (+0.14) compared to the replica. It is important to underline that `j48`, `ibk`, `random forest` and `reptree` had the same performances

3.4. FINAL REMARKS

and `logistic` in contrast to the first case, was the algorithm with the worst performance.

Instead for the last case where both entropies were used, a performance to report is certainly that of the algorithm `bayesnet` with an increment in terms of *MCC* equal to (+0.06). In any case, the experiment in question was placed in the middle between the two previous ones.

Table 3.5: Machine learning algorithms applied on the dataset with explicit and encoded entropy, compared with the replication of Zhou and Zhou, et al [17] itself.

| Dataset | Algorithm | Results | | | | |
|----------|--------------------|--------------|-------|--------|--------|--------------|
| | | SE(%) | SP(%) | PPV(%) | ACC(%) | MCC(%) |
| Explicit | j48 | 96.01 | 97.19 | 96.21 | 96.69 | 93.22 |
| | ibk | 94.95 | 96.09 | 94.74 | 95.60 | 91.01 |
| | logistic | 96.93 | 96.58 | 95.47 | 96.73 | 93.33 |
| | bayesnet | 96.05 | 96.72 | 95.61 | 96.43 | 92.71 |
| | adaboostm1 | 95.57 | 97.34 | 96.39 | 96.59 | 93.01 |
| | randomforest | 95.19 | 96.10 | 94.78 | 95.71 | 91.24 |
| | reptree | 95.38 | 97.32 | 96.36 | 96.49 | 92.83 |
| Encoded | j48 | 96.48 | 97.27 | 96.33 | 96.93 | 93.73 |
| | ibk | 96.48 | 97.27 | 96.33 | 96.93 | 93.73 |
| | logistic | 96.03 | 97.04 | 96.01 | 96.61 | 93.06 |
| | bayesnet | 96.07 | 97.45 | 96.56 | 96.86 | 93.59 |
| | adaboostm1 | 96.03 | 97.53 | 96.66 | 96.89 | 93.64 |
| | randomforest | 96.48 | 97.27 | 96.33 | 96.93 | 93.73 |
| | reptree | 96.48 | 97.27 | 96.33 | 96.93 | 93.73 |
| Both | j48 | 95.98 | 97.19 | 96.21 | 96.68 | 93.20 |
| | logistic | 96.67 | 96.91 | 95.87 | 96.81 | 93.48 |
| | bayesnet | 96.05 | 97.53 | 96.65 | 96.90 | 93.65 |
| | adaboostm1 | 95.57 | 97.34 | 96.39 | 96.59 | 93.01 |
| | randomforest | 95.15 | 96.05 | 94.71 | 95.66 | 91.14 |
| | reptree | 95.32 | 97.28 | 96.31 | 96.45 | 92.73 |
| AFDB | replication | 96.01 | 97.51 | 96.62 | 96.87 | 93.59 |

‘NA’ indicates not applicable because there the metric is not offered by the reference [17].

Without 126 transient values

In 2.3 Shannon entropy has been defined on a bin with size 127. Therefore, to avoid possible interpretations of the state of the art work, the first 126 transient beats were removed, the 127th value it’s completely defined on the previous 126 values, thus it was not removed. The dataset used as a base were the explicit and encoded dataset, because if there are improvements here consequently there are on the experimentations that use them as a starting point. Table 3.6 shows the results obtained.

In the case of the explicit dataset, logistic in terms of *SE* obtained a remarkable increment of (+0.86). But was not enough to compete with the

CHAPTER 3. IMPROVING GLOBAL PREDICTION WITH MORPHOLOGICAL FEATURES

Table 3.6: Machine learning algorithms applied on the dataset with explicit and encoded entropy without the transient beats, compared with the replication of Zhou and Zhou, et al [17, p. 7] itself.

| Dataset | Algorithm | Results | | | | |
|-------------------|--------------------|--------------|-------|--------|--------|--------------|
| | | SE(%) | SP(%) | PPV(%) | ACC(%) | MCC(%) |
| Explicit | j48 | 96.08 | 97.19 | 96.23 | 96.72 | 93.29 |
| | ibk | 94.99 | 96.14 | 94.83 | 95.65 | 91.11 |
| | logistic | 96.97 | 96.60 | 95.50 | 96.76 | 93.40 |
| | bayesnet | 96.12 | 96.73 | 95.64 | 96.47 | 92.79 |
| | adaboostm1 | 95.65 | 97.33 | 96.39 | 96.61 | 93.07 |
| | randomforest | 95.23 | 96.16 | 94.87 | 95.77 | 91.35 |
| | reptree | 95.44 | 97.29 | 96.33 | 96.50 | 92.84 |
| Encoded | j48 | 96.56 | 97.26 | 96.34 | 96.96 | 93.79 |
| | ibk | 96.56 | 97.26 | 96.34 | 96.96 | 93.79 |
| | logistic | 96.11 | 97.53 | 96.66 | 96.92 | 93.71 |
| | bayesnet | 96.13 | 97.45 | 96.57 | 96.89 | 93.64 |
| | adaboostm1 | 96.11 | 97.53 | 96.66 | 96.92 | 93.71 |
| | randomforest | 96.56 | 97.26 | 96.34 | 96.96 | 93.79 |
| | reptree | 96.56 | 97.26 | 96.34 | 96.96 | 93.79 |
| AFDB | replication | 96.01 | 97.51 | 96.62 | 96.87 | 93.59 |
| AFDB ¹ | replication | 96.11 | 97.53 | 96.66 | 96.92 | 93.71 |

¹ dataset without the 126 transient beats.

‘NA’ indicates not applicable because there the metric is not offered by the reference [17].

replica results based on *AFDB*¹. If compared with the results in Table 3.5, an overall slight improvement in terms of *MCC* was achieved and the distance between the replica and the best performance algorithm reduce from (-0.26) to (-0.19) .

As for the encoded dataset, the behaviour was quite similar to what happened in 3.5. In fact, *j48*, *ibk*, *random forest* and *reptree* had the same performances. But *logistic* and *adaboostm1* added nothing more to the replica. In terms of *MCC* compared to the replica, the quartet of algorithms had an increment of around $(+0.08)$. All in all, the experiment without removing the 126 transient beats, obtained greater increments equal to $(+0.14)$ in terms of *MCC*.

3.4. FINAL REMARKS

Table 3.7: Part 1: Records with specific improvements of classification based on encoded entropy with FFT experiment.

| Record | Algorithm | Confusion matrix | | | | Surpasses |
|--------|----------------------|------------------|--------------|-------------|-------------|--------------------------|
| | | TP | TN | FP | FN | |
| 05261 | j48 | 760 | 42459 | 2131 | 174 | <i>Se</i> |
| 05261 | logistic | 682 | 44137 | 453 | 252 | <i>Se</i> |
| 05261 | adaboostm1 | 655 | 44195 | 395 | 279 | <i>Se</i> |
| 05261 | randomforest | 714 | 43248 | 1342 | 220 | <i>Se</i> |
| 05261 | reptree | 768 | 42507 | 2083 | 166 | <i>Se</i> |
| 05261 | Zhou et, al | 654 | 44217 | 380 | 280 | – |
| 07879 | j48 | 39982 | 16222 | 327 | 53 | <i>Se</i> |
| 07879 | logistic | 39945 | 16486 | 63 | 90 | <i>Se</i> |
| 07879 | adaboostm1 | 39945 | 16487 | 62 | 90 | <i>Se</i> |
| 07879 | randomforest | 39963 | 16396 | 153 | 72 | <i>Se</i> |
| 07879 | reptree | 39988 | 15974 | 575 | 47 | <i>Se</i> |
| 07879 | Zhou et, al | 39943 | 16496 | 60 | 92 | – |
| 06453 | j48 | 187 | 22141 | 12241 | 258 | <i>Se</i> |
| 06453 | logistic, adaboostm1 | 126 | 34290 | 92 | 319 | <i>All</i> |
| 06453 | randomforest | 133 | 24539 | 9843 | 312 | <i>Se</i> |
| 06453 | reptree | 165 | 22936 | 11446 | 280 | <i>Se</i> |
| 06453 | Zhou et, al | 117 | 34272 | 117 | 328 | – |
| 04043 | j48 | 8784 | 44373 | 2898 | 5850 | <i>All</i> |
| 04043 | logistic, adaboostm1 | 8693 | 44211 | 3060 | 5941 | <i>Se, Ppv, Acc, Mcc</i> |
| 04043 | randomforest | 8862 | 44493 | 2778 | 5772 | <i>All</i> |
| 04043 | reptree | 8945 | 44110 | 3161 | 5689 | <i>Se</i> |
| 04043 | Zhou et, al | 8544 | 44321 | 2957 | 6090 | – |
| 05091 | j48 | 17 | 34977 | 1650 | 124 | <i>Se</i> |
| 05091 | logistic, adaboostm1 | 0 | 36627 | 0 | 141 | <i>None</i> |
| 05091 | randomforest | 5 | 36346 | 281 | 136 | <i>Se</i> |
| 05091 | reptree | 6 | 34560 | 2067 | 135 | <i>Se</i> |
| 05091 | Zhou et, al | 0 | 36634 | 0 | 141 | – |
| 08405 | j48 | 43452 | 13709 | 42 | 1643 | <i>None</i> |
| 08405 | logistic | 44974 | 13330 | 421 | 121 | <i>None</i> |
| 08405 | adaboostm1 | 45005 | 13751 | 0 | 90 | <i>Acc, Mcc</i> |
| 08405 | randomforest | 44986 | 13742 | 9 | 109 | <i>None</i> |
| 08405 | reptree | 44805 | 13720 | 31 | 290 | <i>None</i> |
| 08405 | Zhou et, al | 45003 | 13758 | 0 | 92 | – |
| 08434 | j48 | 1707 | 35874 | 1656 | 603 | <i>None</i> |
| 08434 | logistic, adaboostm1 | 2310 | 37359 | 171 | 0 | <i>None</i> |
| 08434 | randomforest | 2123 | 36649 | 881 | 187 | <i>None</i> |
| 08434 | reptree | 1667 | 36573 | 957 | 643 | <i>None</i> |
| 08434 | Zhou et, al | 2310 | 37369 | 168 | 0 | – |
| 06995 | j48 | 26854 | 25223 | 2440 | 662 | <i>None</i> |
| 06995 | logistic | 27007 | 25618 | 2045 | 509 | <i>Se, Acc, Mcc</i> |
| 06995 | adaboostm1 | 26975 | 25645 | 2018 | 541 | <i>All</i> |
| 06995 | randomforest | 26948 | 25556 | 2107 | 568 | <i>None</i> |
| 06995 | reptree | 26524 | 25119 | 2544 | 992 | <i>None</i> |
| 06995 | Zhou et, al | 26961 | 25640 | 2023 | 562 | – |
| 04746 | j48 | 30020 | 16882 | 108 | 853 | <i>None</i> |
| 04746 | logistic, adaboostm1 | 30732 | 16894 | 96 | 141 | <i>None</i> |
| 04746 | randomforest | 30552 | 16881 | 109 | 321 | <i>None</i> |
| 04746 | reptree | 29516 | 16892 | 98 | 1357 | <i>None</i> |
| 04746 | Zhou et, al | 30732 | 16902 | 95 | 141 | – |
| 07910 | j48 | 6153 | 29132 | 687 | 617 | <i>None</i> |
| 07910 | logistic, adaboostm1 | 6499 | 29715 | 104 | 271 | <i>None</i> |
| 07910 | randomforest | 6195 | 29503 | 316 | 575 | <i>None</i> |
| 07910 | reptree | 5498 | 29280 | 539 | 1272 | <i>None</i> |
| 07910 | Zhou et, al | 6499 | 29722 | 104 | 271 | – |

CHAPTER 3. IMPROVING GLOBAL PREDICTION WITH MORPHOLOGICAL FEATURES

Table 3.8: Part 2: Records with specific improvements of classification based on encoded entropy with FFT experiment.

| Record | Algorithm | Confusion matrix | | | | Surpasses |
|--------|----------------------|------------------|--------------|-------------|-------------|--------------------------|
| | | TP | TN | FP | FN | |
| 08215 | j48 | 30146 | 10173 | 43 | 2984 | <i>Sp</i> |
| 08215 | logistic, adaboostm1 | 32958 | 10171 | 45 | 172 | <i>None</i> |
| 08215 | randomforest | 32409 | 10175 | 41 | 721 | <i>Sp, Ppv</i> |
| 08215 | reptree | 32118 | 10168 | 48 | 1012 | <i>None</i> |
| 08215 | Zhou et, al | 32958 | 10178 | 45 | 172 | – |
| 04908 | j48 | 5313 | 53909 | 2031 | 497 | <i>None</i> |
| 04908 | logistic | 5446 | 55275 | 665 | 364 | <i>Sp, Ppv, Acc, Mcc</i> |
| 04908 | adaboostm1 | 5446 | 55279 | 661 | 364 | <i>Sp, Ppv, Acc, Mcc</i> |
| 04908 | randomforest | 5348 | 53829 | 2111 | 462 | <i>None</i> |
| 04908 | reptree | 5362 | 53508 | 2432 | 448 | <i>None</i> |
| 04908 | Zhou et, al | 5491 | 55055 | 892 | 319 | – |
| 08455 | j48 | 43737 | 15205 | 73 | 527 | <i>None</i> |
| 08455 | logistic, adaboostm1 | 44102 | 15239 | 39 | 162 | <i>None</i> |
| 08455 | randomforest | 43975 | 15236 | 42 | 289 | <i>None</i> |
| 08455 | reptree | 43884 | 15227 | 51 | 380 | <i>None</i> |
| 08455 | Zhou et, al | 44103 | 15246 | 39 | 161 | – |
| 05121 | j48 | 32613 | 13830 | 2281 | 1147 | <i>None</i> |
| 05121 | logistic, adaboostm1 | 32589 | 14986 | 1125 | 1171 | <i>Sp, Ppv</i> |
| 05121 | randomforest | 32686 | 14478 | 1633 | 1074 | <i>None</i> |
| 05121 | reptree | 32650 | 13115 | 2996 | 1110 | <i>None</i> |
| 05121 | Zhou et, al | 32689 | 14923 | 1195 | 1071 | – |
| 08378 | j48 | 9217 | 33815 | 213 | 2260 | <i>None</i> |
| 08378 | logistic | 10994 | 33441 | 587 | 483 | <i>None</i> |
| 08378 | adaboostm1 | 10996 | 33886 | 142 | 481 | <i>Sp, Ppv</i> |
| 08378 | randomforest | 10108 | 33839 | 189 | 1369 | <i>None</i> |
| 08378 | reptree | 10031 | 33834 | 194 | 1446 | <i>None</i> |
| 08378 | Zhou et, al | 11008 | 33891 | 144 | 469 | – |
| 04015 | j48 | 488 | 39394 | 4076 | 37 | <i>Se</i> |
| 04015 | logistic | 483 | 40787 | 2683 | 42 | <i>None</i> |
| 04015 | adaboostm1 | 483 | 40807 | 2663 | 42 | <i>Sp</i> |
| 04015 | randomforest | 466 | 40650 | 2820 | 59 | <i>None</i> |
| 04015 | reptree | 487 | 39872 | 3598 | 38 | <i>Sp</i> |
| 04015 | Zhou et, al | 485 | 40812 | 2665 | 40 | – |
| 06426 | j48 | 50954 | 731 | 1288 | 2172 | <i>None</i> |
| 06426 | logistic | 52015 | 781 | 1238 | 1111 | <i>None</i> |
| 06426 | adaboostm1 | 52014 | 799 | 1220 | 1112 | <i>Sp, Ppv</i> |
| 06426 | randomforest | 51638 | 797 | 1222 | 1488 | <i>Sp</i> |
| 06426 | reptree | 50734 | 734 | 1285 | 2392 | <i>None</i> |
| 06426 | Zhou et, al | 52095 | 796 | 1223 | 1038 | – |
| 04048 | j48 | 567 | 38838 | 273 | 246 | <i>Se, Acc, Mcc</i> |
| 04048 | logistic | 435 | 38966 | 145 | 378 | <i>Se, Acc, Mcc</i> |
| 04048 | adaboostm1 | 419 | 38974 | 137 | 394 | <i>None</i> |
| 04048 | randomforest | 476 | 38958 | 153 | 337 | <i>Se, Ppv, Acc, Mcc</i> |
| 04048 | reptree | 548 | 38924 | 187 | 265 | <i>Se, Acc, Mcc</i> |
| 04048 | Zhou et, al | 419 | 38982 | 136 | 394 | – |
| 04936 | j48 | 24127 | 12672 | 1283 | 15554 | <i>Sp</i> |
| 04936 | logistic | 34342 | 9273 | 4682 | 5339 | <i>Se</i> |
| 04936 | adaboostm1 | 32834 | 12281 | 1674 | 6847 | <i>Se, Acc, Mcc</i> |
| 04936 | randomforest | 27801 | 12633 | 1322 | 11880 | <i>Sp, Ppv</i> |
| 04936 | reptree | 28221 | 12267 | 1688 | 11460 | <i>None</i> |
| 04936 | Zhou et, al | 32662 | 12362 | 1600 | 7019 | – |

3.4. FINAL REMARKS

Table 3.9: Part 3: Records with specific improvements of classification based on encoded entropy with FFT experiment.

| Record | Algorithm | Confusion matrix | | | | Surpasses |
|--------|--------------|------------------|--------------|-------------|-------------|--------------------------|
| | | TP | TN | FP | FN | |
| 04126 | j48 | 3047 | 37841 | 1716 | 246 | <i>Se</i> |
| 04126 | logistic | 3017 | 38789 | 768 | 276 | <i>Sp</i> |
| 04126 | adaboostm1 | 3017 | 38789 | 768 | 276 | <i>Sp</i> |
| 04126 | randomforest | 3080 | 38508 | 1049 | 213 | <i>Se</i> |
| 04126 | reptree | 3098 | 38210 | 1347 | 195 | <i>Se</i> |
| 04126 | Zhou et, al | 3021 | 38795 | 769 | 272 | — |
| 07162 | j48 | 39161 | 0 | 0 | 127 | <i>None</i> |
| 07162 | logistic | 39198 | 0 | 0 | 90 | <i>Se, Acc</i> |
| 07162 | adaboostm1 | 39198 | 0 | 0 | 90 | <i>Se, Acc</i> |
| 07162 | randomforest | 39198 | 0 | 0 | 90 | <i>Se, Acc</i> |
| 07162 | reptree | 39141 | 0 | 0 | 147 | <i>None</i> |
| 07162 | Zhou et, al | 39198 | 0 | 0 | 97 | — |
| 07859 | j48 | 43752 | 0 | 0 | 18130 | <i>None</i> |
| 07859 | logistic | 61789 | 0 | 0 | 93 | <i>Se, Acc</i> |
| 07859 | adaboostm1 | 61789 | 0 | 0 | 93 | <i>Se, Acc</i> |
| 07859 | randomforest | 51086 | 0 | 0 | 10796 | <i>None</i> |
| 07859 | reptree | 46305 | 0 | 0 | 15577 | <i>None</i> |
| 07859 | Zhou et, al | 61789 | 0 | 0 | 100 | — |
| 08219 | j48 | 12931 | 41354 | 3735 | 1263 | <i>Se</i> |
| 08219 | logistic | 12643 | 42537 | 2552 | 1551 | <i>None</i> |
| 08219 | adaboostm1 | 12643 | 42605 | 2484 | 1551 | <i>Sp, Pre, Acc, Mcc</i> |
| 08219 | randomforest | 12699 | 42199 | 2890 | 1495 | <i>Se</i> |
| 08219 | reptree | 12866 | 41516 | 3573 | 1328 | <i>Se</i> |
| 08219 | Zhou et, al | 12645 | 42555 | 2541 | 1549 | — |

Chapter 4

An adaptive and local prediction approach

Another experiment is attempted to see if it is possible to improve Zhou et, al algorithm using only one characteristic, the threshold of entropy that is variable and adapts to the local characteristics of the patient. A threshold that starts from a standard value, but that over time, when a fibrillation event occurs, adapts to reach an optimal threshold that improves the accuracy of the detection of AF compared to the default threshold.

4.1 Approach description

A `gls` function was used, which fits a linear model using generalized least squares, to find the local optimal threshold. It was performed on an arbitrary observation window of 30 beats with AF and on a window, used in the literature, of 126 AF beats.

4.2 Empirical evaluation

This section describes the datasets and the model used to make predictions. Finally, results obtained are shown.

4.2.1 Design & Context

A dataset to perform a leave one person out experiment was made. It was formed by groups of first 30 beats with atrial fibrillation and their optimal threshold of belonging record. The latter was the label at the base of the supervised learning. A `gls` function was used, which fits a linear model using

generalized least squares. Unfortunately, most of the predicted thresholds were really similar. A further experiment with a time window of 126 heartbeats, a length equal to the state of the art window, was performed but led to almost similar results. Subsequently, validation was carried out, calculating the difference between the above thresholds and the optimal thresholds.

4.2.2 Results

Finding the optimal thresholds

The procedure to complete the task consists of brutally testing all the thresholds in the range $[0.0, 1.0]$ with an increase of 0.001 for every single record. The choice of the right threshold among all the others can be done by optimizing different parameters and metrics (equation 2.5 for reference).

Receiver operating characteristic The ROC was employed to optimize in the same way as Zhou, et al[17] did, but for every single record. To decide if the performances were remarkable, the MCC metric was calculated on the total of the values of the confusion matrix. Then it was compared with the replica realized for the global prevision. On the AFDB dataset the final MCC was 90.05% while the replica's one was 93.59% and the average of all the thresholds was 0.461. Instead, on the AFDB dataset without the 126 transient values, the MCC was 90.12% while the one of the replica was 93.71% and the average threshold 0.522. In both cases, the optimisation carried out was not sufficient to achieve good performance.

Maximizing the number of TP and TN In this trial, the optimization was directed on the number of beats correctly classified, i.e., true positives and true negatives. That is to find that threshold with the highest accuracy (*ACC*). This method on the AFDB dataset yield to an aggregate MCC of 95.00% compared to the 93.59% of the replica. In this case, the threshold average lied around 0.578. On the other hand, the AFDB reduced of the 126 transient beats, had an MCC of 95.04% while the replica 93.71%. The average of the threshold was 0.637. This method was indeed the best one (Table 4.1) and resulting thresholds from the records without the transient beats were used as labels for the dataset.

Validation The final validation was made by making the difference between the thresholds predicted by the GLS model and the optimal thresholds. Results reported in Table 4.2.

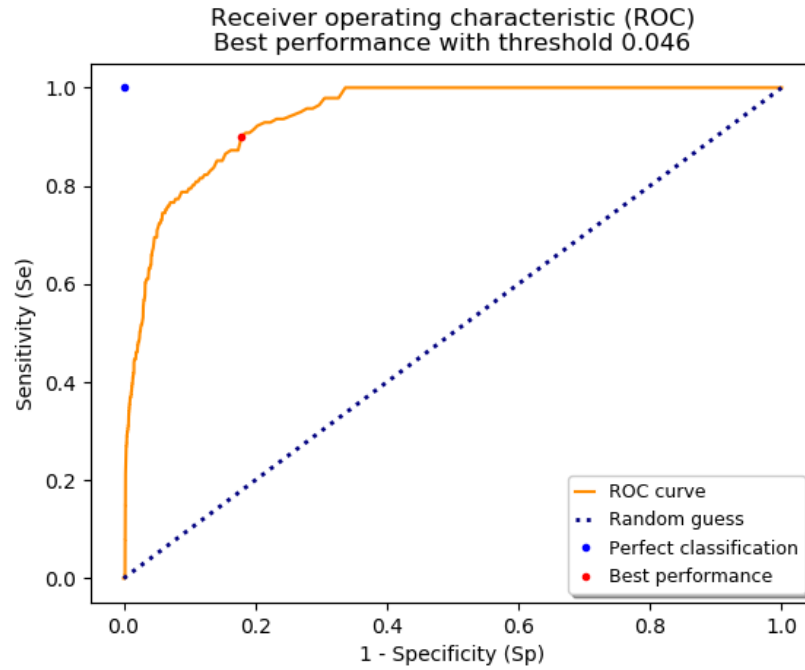


Figure 4.1: Example of optimisation through ROC. For the record 05091, the best performance is obtained with threshold 0.046. $Se = 0.90$ and $Sp = 0.82$.

4.3 Final remarks

For a large number of records, the prediction approaches the optimal threshold. For others, however, there is a significant difference, so other algorithms must be used. Possible methods that might prove interesting are genetic algorithms that are more complex than linear regression.

4.3. FINAL REMARKS

Table 4.1: Summary of local prediction best threshold per record.

| Method | Dataset | MCC | Threshold average |
|---------|-------------------|--------|-------------------|
| ROC | AFDB | 90.05% | 0.461 |
| ROC | AFDB ¹ | 90.12% | 0.461 |
| TP & TN | AFDB | 95.00% | 0.578 |
| TP & TN | AFDB ¹ | 95.04% | 0.637 |
| Replica | AFDB | 93.59% | 0.639 |
| Replica | AFDB ¹ | 93.71% | 0.639 |

¹ AFDB without the 126 transient beats.

Table 4.2: GLS function applied on a dataset with a window of the first 30 AF beats. The output of the function is a threshold.

| Record | Optimal threshold | Predicted threshold | Difference |
|--------|-------------------|---------------------|------------|
| 00735 | 0.632 | 0.5490468 | 0.08295317 |
| 03665 | 0.713 | 0.5397742 | 0.1732258 |
| 04015 | 0.999 | 0.5435027 | 0.4554973 |
| 04043 | 0.515 | 0.5476209 | 0.03263931 |
| 04048 | 0.979 | 0.5394849 | 0.4395151 |
| 04126 | 0.899 | 0.5246542 | 0.3743458 |
| 04746 | 0.471 | 0.5518012 | 0.08080118 |
| 04908 | 0.693 | 0.5429615 | 0.1500385 |
| 04936 | 0.514 | 0.5499928 | 0.03600446 |
| 05091 | 1 | 0.5503535 | 0.4496465 |
| 05121 | 0.557 | 0.5460103 | 0.01135475 |
| 05261 | 0.758 | 0.5456952 | 0.2123048 |
| 06426 | 0.576 | 0.5437635 | 0.03224319 |
| 06453 | 0.726 | 0.5489861 | 0.1770139 |
| 06995 | 0.75 | 0.5348914 | 0.2151086 |
| 07162 | 0.803 | 0.4498696 | 0.3531304 |
| 07859 | 0.687 | 0.5280188 | 0.1589812 |
| 07879 | 0.489 | 0.5547526 | 0.06575262 |
| 07910 | 0.47 | 0.548922 | 0.07892204 |
| 08215 | 0.197 | 0.6375596 | 0.4405596 |
| 08219 | 0.623 | 0.5442554 | 0.07874457 |
| 08378 | 0.354 | 0.5520026 | 0.1980026 |
| 08405 | 0.632 | 0.5341969 | 0.09780312 |
| 08434 | 0.71 | 0.5460842 | 0.1639158 |
| 08455 | 0.199 | 0.6039946 | 0.4049946 |

Chapter 5

Conclusions

5.1 Final remarks

The thesis highlights the danger of atrial fibrillation and how there is a need for automatic tools that can detect it and allows to avoid in some cases much more serious diseases. Several works in the literature try to define automatic instruments, some are based on the irregularity of the *RR* segments, others on the rhythm of the heartbeat. The thesis is based on the latter.

Two approaches are proposed to improve the state of the art considered.

1. The first approach at a global level seeks to improve the number of fibrillating and non-fibrillating beats, correctly classified, by using machine learning techniques to be applied on datasets enriched with morphological features, such as Fourier fast transform and AR coefficients. In this case, considerable improvements on some records were obtained.
2. The second approach, on the other hand, imposes the objective of finding an optimal threshold that adapts in real-time, working exclusively on the threshold. The results are promising because they are very close to the optimal threshold, but still need to be improved.

5.2 Future works

Future work will focus on improving individual approaches in a totally independent manner. In the first case, experiment with neural networks. In the second case, try to use genetic algorithms to improve the prediction of local thresholds. The next step could be to experiment with an adaptive approach on a global model. That is, to adapt the threshold taking into account what is the morphology of the patient.

Bibliography

- [1] Atrial fibrillation fact sheet|data & statistics|dhdsp|cdc, Aug 2017.
- [2] Philip A. Wolf, Robert D. Abbott, and William B. Kannel. Atrial Fibrillation: A Major Contributor to Stroke in the Elderly: The Framingham Study. *Archives of Internal Medicine*, 147(9):1561–1564, 09 1987.
- [3] Thomas M. Munger, Li-Qun Wu, and Win K. Shen. Atrial fibrillation. *Journal of biomedical research*, 28(1):1–17, Jan 2014. 24474959[pmid].
- [4] Sumeet S. Chugh, Rasmus Havmoeller, Kumar Narayanan, David Singh, Michiel Rienstra, Emelia J. Benjamin, Richard F. Gillum, Young-Hoon Kim, John H. McAnulty, Zhi-Jie Zheng, Mohammad H. Forouzanfar, Mohsen Naghavi, George A. Mensah, Majid Ezzati, and Christopher J.L. Murray. Worldwide epidemiology of atrial fibrillation. *Circulation*, 129(8):837–847, 2014.
- [5] Types of atrial fibrillation: Persistent, paroxysmal & permanent afib, Jun 2018.
- [6] H. S. Abed and G. A. Wittert. Obesity and atrial fibrillation. *Obesity Reviews*, 14(11):929–938, 2013.
- [7] David Tonelo, Rui Providência, and Lino Gonçalves. Holiday heart syndrome revisited after 34 years. *Arquivos brasileiros de cardiologia*, 101(2):183–189, Aug 2013. 24030078[pmid].
- [8] Xin Du, Jianzeng Dong, and Changsheng Ma. Is atrial fibrillation a preventable disease? *Journal of the American College of Cardiology*, 69(15):1968 – 1982, 2017.
- [9] Caroline S. Fox, Helen Parise, Ralph B. D’Agostino, Sr, Donald M. Lloyd-Jones, Ramachandran S. Vasan, Thomas J. Wang, Daniel Levy, Philip A. Wolf, and Emelia J. Benjamin. Parental Atrial Fibrillation as a Risk Factor for Atrial Fibrillation in Offspring. *JAMA*, 291(23):2851–2855, 06 2004.

- [10] Laila Staerk, Jason A. Sherer, Darae Ko, Emelia J. Benjamin, and Robert H. Helm. Atrial fibrillation: Epidemiology, pathophysiology, and clinical outcomes. *Circulation research*, 120(9):1501–1517, Apr 2017. 28450367[pmid].
- [11] Ernest Noble Chamberlain, David Gray, and Andrew R. Houghton. *Chamberlains symptoms and signs in clinical medicine: an introduction to medical diagnosis*. Hodder Arnold, 2010.
- [12] Richard L Page, Thomas W Tilsch, Stuart J Connolly, Daniel J Schnell, Stephen R Marcello, William E Wilkinson, and Edward LC Pritchett. Asymptomatic or “silent” atrial fibrillation: frequency in untreated patients and patients receiving azimilide. *Circulation*, 107(8):1141–1145, 2003.
- [13] Atrial fibrillation, Jun 2019.
- [14] L.S. Lilly and Harvard Medical School. *Pathophysiology of Heart Disease: A Collaborative Project of Medical Students and Faculty*, page 74. Wolters Kluwer, 2015.
- [15] Valentin Fuster, Lars E. Rydén, David S. Cannom, Harry J. Crijns, Anne B. Curtis, Kenneth A. Ellenbogen, Jonathan L. Halperin, Jean-Yves Le Heuzey, G. Neal Kay, James E. Lowe, S. Bertil Olsson, Eric N. Prystowsky, Juan Luis Tamargo, Samuel Wann, null null, Sidney C. Smith, Alice K. Jacobs, Cynthia D. Adams, Jeffery L. Anderson, Elliott M. Antman, Jonathan L. Halperin, Sharon Ann Hunt, Rick Nishimura, Joseph P. Ornato, Richard L. Page, Barbara Riegel, null null, Silvia G. Priori, Jean-Jacques Blanc, Andrzej Budaj, A. John Camm, Veronica Dean, Jaap W. Deckers, Catherine Despres, Kenneth Dickstein, John Lekakis, Keith McGregor, Marco Metra, Joao Morais, Ady Osterspey, Juan Luis Tamargo, and José Luis Zamorano. Acc/aha/esc 2006 guidelines for the management of patients with atrial fibrillation. *Circulation*, 114(7):e257–e354, 2006.
- [16] Z.F. Issa, J.M. Miller, and D.P. Zipes. *Clinical Arrhythmology and Electrophysiology: A Companion to Braunwald’s Heart Disease*, page 221. Companion to Braunwald’s Heart Disease Series. Saunders, 2009.
- [17] Xiaolin Zhou, Hongxia Ding, Wanqing Wu, and Yuanting Zhang. A real-time atrial fibrillation detection algorithm based on the instantaneous state of heart rate. *PLOS ONE*, 10(9):1–16, 09 2015.

BIBLIOGRAPHY

- [18] A. L. Goldberger, L. A. Amaral, L. Glass, J. M. Hausdorff, P. C. Ivanov, R. G. Mark, J. E. Mietus, G. B. Moody, C. K. Peng, and H. E. Stanley. PhysioBank, PhysioToolkit, and PhysioNet: components of a new research resource for complex physiologic signals. *Circulation*, 101(23):E215–220, Jun 2000.
- [19] G. MOODY. A new method for detecting atrial fibrillation using r-r intervals. *Computers in Cardiology*, pages 227–230, 1983.
- [20] Simona Petrutiu, Alan V. Sahakian, and Steven Swiryn. Abrupt changes in fibrillatory wave characteristics at the termination of paroxysmal atrial fibrillation in humans. *EP Europace*, 9(7):466–470, 05 2007.
- [21] Andrius Petrėnas, Vaidotas Marozas, and Leif Sörnmo. Low-complexity detection of atrial fibrillation in continuous long-term monitoring. *Computers in biology and medicine*, 65:184–191, 2015.
- [22] J. Lee, Y. Nam, D. D. McManus, and K. H. Chon. Time-varying coherence function for atrial fibrillation detection. *IEEE Transactions on Biomedical Engineering*, 60(10):2783–2793, Oct 2013.
- [23] Xiaolin Zhou, Hongxia Ding, Benjamin Ung, Emma Pickwell-MacPherson, and Yuanting Zhang. Automatic online detection of atrial fibrillation based on symbolic dynamics and shannon entropy. *BioMedical Engineering OnLine*, 13(1):18, 2014.